Chapter 15:
Evaluation of the Numerical Results

B. Koren
CWI
P.O. Box 4079, 1009 AB Amsterdam, The Netherlands

C.B. Vreugdenhil
IMAU
P.O. Box 80.005, 3508 TA Utrecht, The Netherlands

15.1 Introduction

In this chapter, quantitative and qualitative comparisons are made between the various *discretization* methods, as described and tested in Chapters 2-11. The comparisons are made on the basis of the numerical results obtained for the problems prescribed in Chapter 1. The *solution* methods considered in Chapters 12-14 are not evaluated here. We think that these three chapters are sufficiently surveyable to be evaluated by the readers themselves.

We start by making quantitative comparisons between the discretization methods. For this purpose, we have in principle selected a single discretization method per chapter. The selected methods are compared on the basis of the numerical results presented for Problem 4. Reliable quantitative comparisons are possible for this problem, because of its smoothness, its well-specified output data, its prescribed sequence of grids: $\sim (20 \times 20), \sim (40 \times 40), \sim (80 \times 80)$, and because of its prescribed benchmark problem for measuring computing times. After this quantitative comparison, partly quantitative - partly qualitative comparisons are made on the basis of the numerical results obtained for Problems 1, 2, 3.1, and 3.2. For these comparisons, per problem we have in principle also selected a single discretization method from each chapter. Interesting difficulties of the latter four problems are the local non-smoothnesses in initial solutions and source terms. These non-smoothnesses may result in reduced global orders of accuracy.

The present evaluation still reflects our own subjective opinions, be it to a minimal extent. We have aimed at objectivity by giving each chapter author the opportunity to make critical reviews of a draft of the present evaluation.

15.2 Evaluation numerical results Problem 4

The various types of discretization methods considered in the preceding chapters, are given in Table 15.1. The specific discretization methods selected for the present (quantitative) evaluation, are given in Table 15.2. For the Chapters 5, 7, 9, and 10, a selection was not necessary; in these chapters, results for Problem 4 are presented for a single method solely. From Chapter 3, because of the rather widely divergent, linear upwind

methods considered in it, two specific schemes have been selected: the skew-triangle scheme and a cyclic scheme.

Table 15.1: Types of discretization methods considered in previous chapters

Chapter	*author(s)*	*method(s)*
2	Vreugdenhil	linear, central finite differences (standard second-order and compact higher-order)
3	Van Eijkeren, De Haan, Stelling, Van Stijn	linear, upwind finite differences (grid-aligned and rotated) and upwind finite volumes
4	Pourquié	classical nonlinear, upwind finite volumes
5	Koren	modern nonlinear, upwind finite volumes
6	Walsteijn	ENO, finite differences (standard and variable order)
7	Timmermans, Van de Vosse	spectral (standard spectral and spectral elements)
8	Segal	finite elements (standard Galerkin and streamline upwind Petrov-Galerkin)
9	Van Eijkeren	backward semi-Lagrangian
10	De Kok	forward semi-Lagrangian
11	Struijs	fluctuation-splitting

Table 15.2: Specific discretization methods to be evaluated for Problem 4

method	*Figure/Table*
leap-frog	Figure 2.9
skew-triangle	Table 3.6
cyclic	Table 3.8
MFCT	Tables 4.4-4.7
limited - $\kappa = \frac{1}{3}$	Table 5.3
ENO-4-LF	Table 6.3b
SEM	Table 7.6
SGA/CN-consistent	Table 8.3
adjoint-equation	Table 9.11
second-moment	Table 10.1
narrow	Figure 11.17

The numerical properties to be evaluated are successively: accuracy (both plain accuracy and accuracy in relation to computational efficiency), positivity and conservation. We realize that this choice of numerical properties does not permit a general evaluation. For this, many more properties should be considered: memory use, complexity of implementation, suitability for parallelization and vectorization, applicability of acceleration techniques (such as conjugate gradients and multigrid), suitability for unstructured grids, and so on. In order to make a clear comparison, we restrict ourselves to the few but relevant numerical properties mentioned before.

Plain accuracy is evaluated on the basis of the numerical data obtained for:

$$|1 - c_{\max}| \equiv |1 - (c_{\text{numerical}}(i,j))_{\max}|\,, \tag{15.1a}$$

$$\|\Delta c\|_1 \equiv \frac{\sum_{i,j} \mid c_{\text{exact}}(i,j) - c_{\text{numerical}}(i,j) \mid}{\sum_{i,j} 1}, \tag{15.1b}$$

$$\|\Delta c\|_\infty \equiv \mid c_{\text{exact}}(i,j) - c_{\text{numerical}}(i,j) \mid_{\max}. \tag{15.1c}$$

Accuracy in relation to computational efficiency is studied by means of $\|\Delta c\|_1$ versus normalized CPU-time. Positivity and conservation are studied by, respectively:

$$|c_{\min}| \equiv |(c_{\text{numerical}}(i,j))_{\min}|\,, \tag{15.2}$$

and

$$|1 - r_{\text{mass}}| \equiv \left|1 - \frac{\sum_{i,j} c_{\text{numerical}}(i,j)}{\sum_{i,j} c_{\text{exact}}(i,j)}\right|. \tag{15.3}$$

All numerical results, except those of the spectral-element scheme, have been obtained on a sequence of three grids with as minimal numbers of points (or cells): $(n_x \times n_y) = (20 \times 20), (40 \times 40), (80 \times 80)$, and with as maximal numbers: $(n_x \times n_y) = (22 \times 21), (42 \times 41), (82 \times 81)$. The fineness of the sequence of three space discretizations as used by the spectral-element method, $(n_e, n) = (4,4), (4,8), (4,16)$, can be considered to be equivalent to that of the grid sequence $(n_x \times n_y) = (9 \times 9), (17 \times 17), (33 \times 33)$. Another remark that needs to be made in advance concerns the treatment of the velocity field by the semi-Lagrangian methods from the Chapters 9 and 10. Both methods use exact characteristic information. (The adjoint-equation method from Chapter 9 directly uses the exact characteristics. The second-moment method from Chapter 10 uses a numerical method in computing the characteristics, but for the present steady, solid-body-like rotation, this numerical method boils down to the use of exact characteristic information as well.) The possibility to use exact characteristic information, if available, definitely is an advantage over Eulerian discretization methods. However, in general, exact information is lacking and it is not sufficiently clear to what extent this absence will detract from the accuracy and computational efficiency of semi-Lagrangian methods.

15.2.1 Plain accuracy

Peak resolution. Peak resolution is measured on the basis of $|1 - c_{\max}|$. Its values, as measured for the selected discretization methods (Table 15.2), are given in Figure 15.1. Per method we depict in upward direction: the values measured on the coarsest, the medium-sized and the finest grid. In addition, in Table 15.3, we give per method the average error value $\overline{|1 - c_{\max}|}$ over the three grids. In case of $(n_x \times n_y) = (20 \times 20), (40 \times 40), (80 \times 80)$, this means $\overline{|1 - c_{\max}|} = \frac{1}{3}\left(|1 - c_{\max}|_{(n_x \times n_y)=(20\times 20)} + |1 - c_{\max}|_{(n_x \times n_y)=(40\times 40)} + |1 - c_{\max}|_{(n_x \times n_y)=(80\times 80)}\right)$. To be able to make a reasonable comparison, for the spectral-element scheme we take $\overline{|1 - c_{\max}|} = \frac{1}{2}\left(|1 - c_{\max}|_{(n_e,n)=(4,8)} + |1 - c_{\max}|_{(n_e,n)=(4,16)}\right)$. (For $\overline{\|\Delta c\|_\infty}$, $\overline{\|\Delta c\|_1}$, $\overline{|c_{\min}|}$ and $\overline{|1 - r_{\text{mass}}|}$, the same averagings will be made.) Furthermore, in Table 15.3 we give the orders of accuracy p (p from $\mathcal{O}(h^p)$), as measured from the medium-sized grid to the finest grid. (In the following, this way of measuring orders of accuracy will also be applied to $\|\Delta c\|_\infty$, $\|\Delta c\|_1$, $|c_{\min}|$, and $|1 - r_{\text{mass}}|$.) With respect to both error level and error convergence, the methods have been ordered in Table 15.3 with increasing performance in upward direction. Moreover, by means of horizontal lines, a

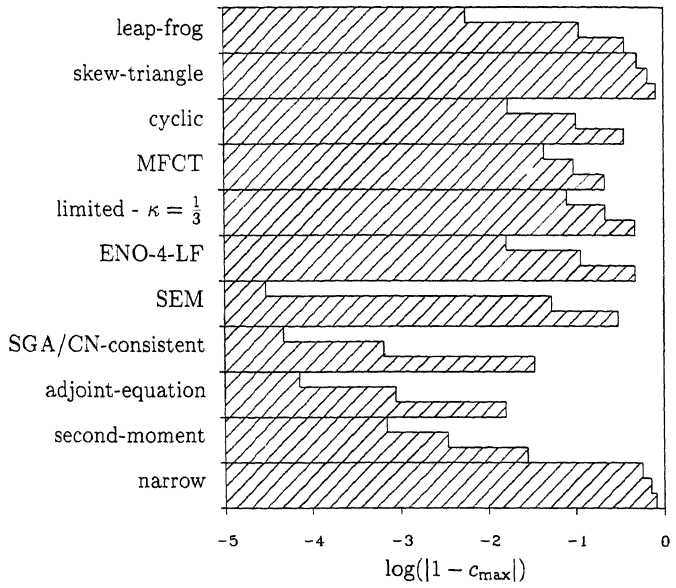

Figure 15.1: Values of $|1 - c_{\max}|$, for prescribed grid sequence and selected discretization methods

Table 15.3: Classifications of discretization methods with respect to $|1 - c_{\max}|$

error level		*error convergence*	
method	$\overline{|1 - c_{\max}|}$	*method*	p
adjoint-equation	0.006	SEM	10.8
second-moment	0.011	leap-frog	4.3
SGA/CN-consistent	0.012	SGA/CN-consistent	3.8
SEM	0.027	adjoint-equation	3.6
MFCT	0.119	ENO-4-LF	2.8
cyclic	0.159	cyclic	2.6
leap-frog	0.161	second-moment	2.3
ENO-4-LF	0.204	limited - $\kappa = \frac{1}{3}$	1.5
limited - $\kappa = \frac{1}{3}$	0.260	MFCT	1.1
skew-triangle	0.667	skew-triangle	0.4
narrow	0.707	narrow	0.3

classification has been made into three categories, say: (i) less good, (ii) good, and (iii) very good. (This type of classification will also be applied to the other four errors.)

We here classify schemes which still have a peak decrease of more than 10 % on the finest grid as low-accurate. We see there are two such schemes: the narrow scheme and the skew-triangle scheme. Concerning the order of accuracy with respect to $|1 - c_{\max}|$, we see that for both schemes this is still below the (theoretically expected) asymptotic $\mathcal{O}(h)$ convergence. Note, however, that for steady multi-D problems the narrow scheme, and particularly the associated PSI scheme, perform significantly better than for unsteady problems (see Chapter 11 for evidence on this.) Probably this relatively better performance for steady problems also holds for the skew-triangle scheme. Good results are obtained by the MFCT scheme and the limited - $\kappa = \frac{1}{3}$ scheme, for error level as well as for error convergence. (With respect to average error level, the MFCT scheme is preferable to the limited - $\kappa = \frac{1}{3}$ scheme, with respect to order behavior it is the reverse.) On average, both methods behave more or less the same. Given the common numerical recipes in the two methods, this was to be expected. Good to very good orders of accuracy are obtained by the two semi-Lagrangian schemes, the cyclic scheme, the ENO scheme, the finite-element scheme, the leap-frog scheme, and the spectral-element scheme. All seven methods have a higher than $\mathcal{O}(h^2)$ accuracy behavior, particularly the spectral-element scheme has a very high order of accuracy. It is followed at great distance by the leap-frog scheme, which is closely followed by the finite-element scheme, the latter having the additional advantage (over the leap-frog scheme) of a very small average error level. As for the superior average peak resolution of the adjoint-equation method, it is unfortunately not clear to what extent this is favored by the direct use of exact characteristic information. The remaining results speak for themselves.

L_∞-norm solution error. We proceed by considering $\|\Delta c\|_\infty$, which for many methods is supposed to be closely related to $|1 - c_{\max}|$. The values of $\|\Delta c\|_\infty$, as measured for the selected methods, are given in Figure 15.2. As in Figure 15.1, depicted upward per method are: the values measured on the coarsest, the medium-sized and the finest grid. Furthermore, as in Table 15.3, in Table 15.4 we also give the classifications for average error levels and orders of accuracy.

The skew-triangle scheme and the narrow scheme appear to behave much the same again. Here also, the orders of accuracy of both schemes are still below $\mathcal{O}(h)$. Good order behavior is shown by the MFCT scheme, the limited - $\kappa = \frac{1}{3}$ scheme, the leap-frog scheme, the adjoint-equation scheme, and the cyclic scheme. All five schemes behave in between $\mathcal{O}(h)$ and $\mathcal{O}(h^2)$. Note the excellent average error level of the adjoint-equation method. Higher than second-order accuracy is shown again by the second-moment scheme, the ENO scheme, the finite-element scheme, and (the best again) by the spectral-element scheme.

L_1-norm solution error. We end this evaluation of plain accuracy by considering $\|\Delta c\|_1$. The values measured for it are given in Figure 15.3. Classifications are given in Table 15.5.

We observe that here also the skew-triangle scheme and the narrow scheme have an order of accuracy which is still lower than $\mathcal{O}(h)$, with the skew-triangle scheme again converging slightly better than the narrow scheme. A nearly $\mathcal{O}(h^2)$ accuracy behavior is obtained by the cyclic scheme and the second-moment scheme. All remaining schemes show a higher than $\mathcal{O}(h^2)$ behavior. A superior order of accuracy is shown again by the

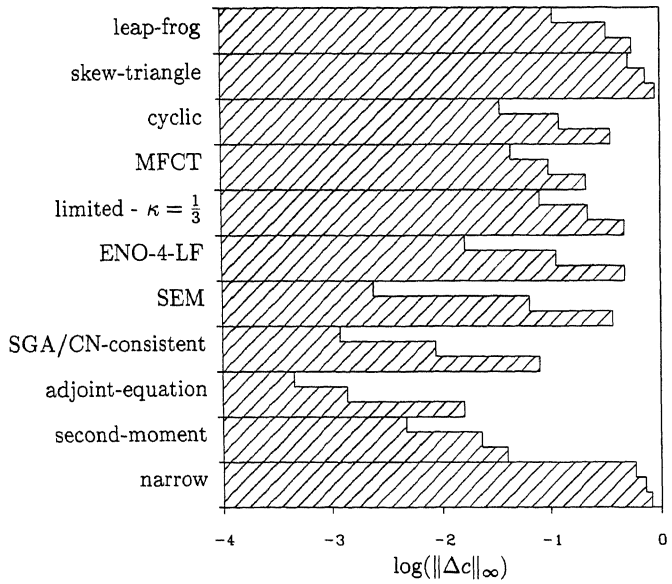

Figure 15.2: Values of $\|\Delta c\|_\infty$, for prescribed grid sequence and selected discretization methods

Table 15.4: Classifications of discretization methods with respect to $\|\Delta c\|_\infty$

error level		*error convergence*	
method	$\overline{\|\Delta c\|_\infty}$	*method*	p
adjoint-equation	0.006	SEM	4.8
second-moment	0.023	SGA/CN-consistent	2.9
SGA/CN-consistent	0.030	ENO-4-LF	2.8
SEM	0.034	second-moment	2.3
MFCT	0.119	cyclic	1.8
cyclic	0.172	leap-frog, adjoint-equation	1.6
ENO-4-LF	0.204	limited - $\kappa = \frac{1}{3}$	1.5
limited - $\kappa = \frac{1}{3}$	0.261	MFCT	1.2
leap-frog	0.333	skew-triangle	0.5
narrow	0.710	narrow	0.3
skew-triangle	0.723		

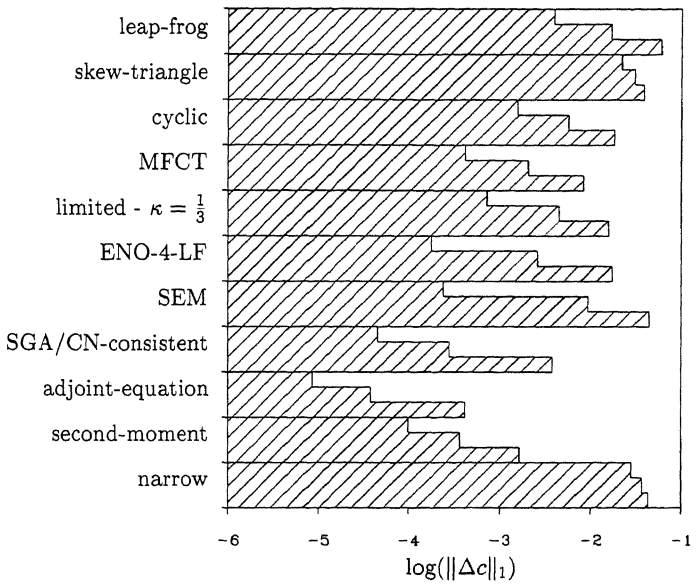

Figure 15.3: Values of $\|\Delta c\|_1$, for prescribed grid sequence and selected discretization methods

Table 15.5: Classifications of discretization methods with respect to $\|\Delta c\|_1$

error level		*error convergence*	
method	$\overline{\|\Delta c\|_1}$	*method*	p
adjoint-equation	1.5×10^{-4}	SEM	5.3
second-moment	7.0×10^{-4}	ENO-4-LF	3.9
SGA/CN-consistent	1.4×10^{-3}	limited - $\kappa = \frac{1}{3}$, SGA/CN-consistent	2.6
MFCT	3.6×10^{-3}	MFCT	2.3
SEM	4.8×10^{-3}	adjoint-equation	2.2
ENO-4-LF	6.7×10^{-3}	leap-frog	2.1
limited - $\kappa = \frac{1}{3}$	7.0×10^{-3}	cyclic, second-moment	1.9
cyclic	8.6×10^{-3}	skew-triangle	0.5
leap-frog	2.7×10^{-2}	narrow	0.4
skew-triangle	3.0×10^{-2}		
narrow	3.6×10^{-2}		

spectral-element scheme. The solution error of the limited - $\kappa = \frac{1}{3}$ scheme converges a little faster again than that of the MFCT scheme, whereas the average error level of the MFCT scheme is somewhat lower again than that of the limited - $\kappa = \frac{1}{3}$ scheme. The ENO scheme practically reaches its $\mathcal{O}(h^4)$ accuracy behavior in going from the medium-sized grid to the finest grid. Yet, note the modest error level of the ENO scheme on the coarsest grid. High-resolution schemes as this ENO scheme (and in some sense also the limited - $\kappa = \frac{1}{3}$ scheme) seem to need sufficient smoothness and distance from boundaries; i.e. sufficient grid fineness. However, note also that this does *not* seem to be the case for the variable-order ENO schemes introduced in Chapter 6 (not depicted in Figure 15.3), nor for the spectral-element scheme (Figure 15.3). (Concerning the variable-order ENO scheme, compare its coarsest-grid value of $\|\Delta c\|_1$, as given in Table 6.6, with the corresponding ENO-4-LF value given in Table 6.3b. As for the spectral-element scheme, we emphasize again that its results for the medium-sized resolution $(n_e, n) = (4, 8)$ should be compared with the coarsest-grid results of all other methods $(n_x \times n_y) \approx (20 \times 20)$.) Excellent coarse-grid resolution is also shown by the Galerkin finite-element scheme and by the two semi-Lagrangian schemes. For the latter two schemes, this can probably be attributed in large measure to their use of exact characteristic information; for the finite-element scheme it is not well-understood, however.

15.2.2 Accuracy versus computational efficiency

Accuracy in relation to computational costs is studied by means of the $\|\Delta c\|_1$-values and normalized CPU-times. Normalization of CPU-times measured by the different authors, has been achieved by means of a benchmark code, the code for the computation of Problem 4 on a 40 × 40-grid, by the leap-frog method from Chapter 2. Since the authors have used different time integrators which also differ in degree of optimization, the importance of the present evaluation should not be overestimated of course. Still we think that the results do give some reliable qualitative information about the price-performance aspects of the various space discretization methods.

In Figure 15.4 the results are given. The measured data of the two semi-Lagrangian schemes (the adjoint-equation method and the second-moment method) as well as the data of the narrow scheme have been set apart from those of the other schemes by connecting them with dashed lines. The narrow scheme differs from the other schemes because it has been implemented in a research code meant for unstructured grids, and the two semi-Lagrangian schemes differ because their use of exact characteristic information influences both accuracy and computational efficiency in a positive way. Ignoring this advantage of semi-Lagrangian schemes for (at least) the present sequence of grids, the two schemes definitely appear to be the best buy. Clearly the best performance of all remaining Eulerian schemes is obtained by the cyclic scheme. It is followed by a cluster of higher than first-order Eulerian methods. From these, the limited - $\kappa = \frac{1}{3}$ scheme and the finite-element scheme perform best. The best scheme for grids finer than the present ones seems to be the spectral-element scheme. It appears that, for perfectly smooth problems, a very high order of spatial accuracy is really useful on finer grids (with the restriction, of course, that the accuracy in time is of very high order as well). Also noteworthy is the performance for grids which are *coarser* than those of the sequence considered here. For these coarse grids, the price-performance behavior of low-order schemes, such as the skew-triangle scheme, becomes interesting. This is relevant for e.g. multigrid computations.

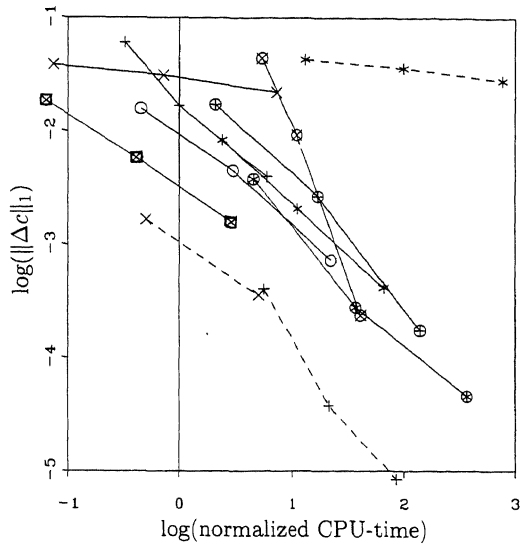

Figure 15.4: Values of $||\Delta c||_1$ versus normalized CPU-times for prescribed grid sequence and selected discretization methods; **solid lines**: +: leap-frog, ×: skew-triangle, ⊠: cyclic, ∗: MFCT, ○: limited - $\kappa = \frac{1}{3}$, ⊕: ENO-4-LF, ⊗: SEM, ⊛: SGA/CN-consistent; **dashed lines**: +: adjoint-equation, ×: second-moment, ∗: narrow

15.2.3 Positivity

Positivity is evaluated on the basis of $|c_{\min}|$. The values of $|c_{\min}|$, as measured on the sequence of grids for the selected discretization methods, are given in Figure 15.5. (In Figure 15.5, no results are missing; all invisible results are smaller than 10^{-10}.) Classifications are given in Table 15.6.

Relatively poor order behavior is shown by the finite-element scheme. A poor average error level is obtained by the leap-frog scheme, closely followed by the spectral-element scheme and the cyclic scheme. Good average error levels are obtained by the limited - $\kappa = \frac{1}{3}$ scheme and the adjoint-equation method, whereas their orders of convergence may even be qualified as very good. The limited - $\kappa = \frac{1}{3}$ scheme is not perfectly positive because it is not applied near boundaries. (By introducing a single row of virtual cells across the boundaries, and then applying the limited scheme up to and including the boundaries, perfectly positive results would be obtained.) Although their order behaviors with decreasing mesh size are not visible, we assume that for sufficiently small time steps, perfect positivity is guaranteed for the four schemes with $|c_{\min}| < 10^{-10}$. (For the skew-triangle scheme and the narrow scheme, this is certainly the case.) In conclusion, we emphasize that the present problem is in fact not very discriminating with respect to the positivity property; more discriminating are Problem 3.1 and - particularly - Problem 3.2 (to be evaluated in the Sections 15.3.3 and 15.3.4).

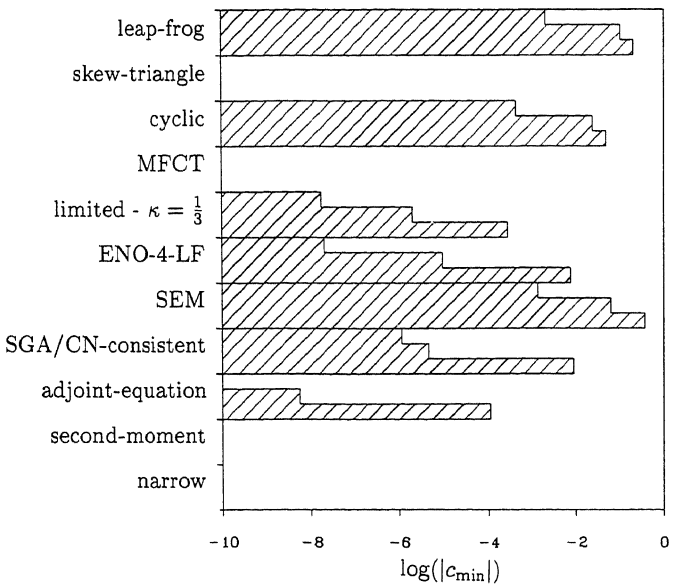

Figure 15.5: Values of $|c_{\min}|$, for prescribed grid sequence and selected discretization methods

Table 15.6: Classifications of discretization methods with respect to $|c_{\min}|$

error level		*error convergence*	
method	$\overline{\lvert c_{\min}\rvert}$	*method*	p
skew-triangle, MFCT, second-moment, narrow	$< 10^{-10}$	ENO-4-LF	8.9
		limited - $\kappa = \frac{1}{3}$	6.9
adjoint-equation	3.7×10^{-5}	cyclic, adjoint-equation	5.8
limited - $\kappa = \frac{1}{3}$	9.4×10^{-5}	leap-frog	5.6
ENO-4-LF	2.6×10^{-3}	SEM	5.5
SGA/CN-consistent	3.0×10^{-3}	SGA/CN-consistent	2.0
cyclic	2.5×10^{-2}		
SEM	3.3×10^{-2}		
leap-frog	1.0×10^{-1}		

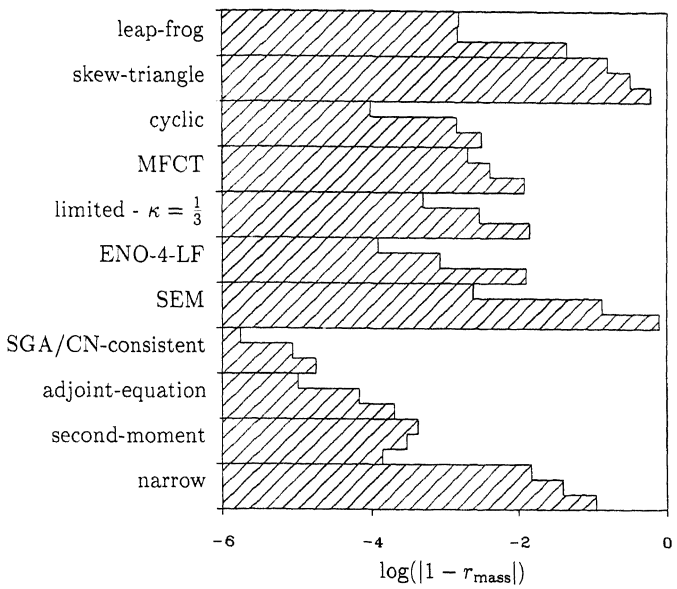

Figure 15.6: Values of $|1 - r_{\text{mass}}|$, for prescribed grid sequence and selected discretization methods

15.2.4 Conservation

Whereas the exact net flux across the entire boundary is zero, the local fluxes are not. Although very small, at (almost) all boundary points there is an inflow or outflow flux. As a consequence, when in a numerical computation the exact fluxes are imposed as inflow boundary conditions and when - mathematically correct - no outflow boundary conditions are imposed, due to discretization errors, the net flux across the entire boundary generally will not be equal to zero. Hence, schemes which are strictly conservative, do not show strictly conservative behavior for this test case, unless - mathematically incorrect - the exact fluxes are also imposed at outflow. Nevertheless, poor conservation properties *can* be detected; for schemes which converge well with respect to $\|\Delta c\|_1$ but not so well with respect to $|1 - r_{\text{mass}}|$, it may be concluded that they have poor conservation properties. For a well-conservative scheme, $|1 - r_{\text{mass}}|$ should converge better, the same, or a little bit worse than $\|\Delta c\|_1$, but *not* much (say one or more orders) worse. Hence, a good quantity to look at here is the measured order of accuracy of $|1 - r_{\text{mass}}|$ subtracted by the corresponding measured order of $\|\Delta c\|_1$. The values of $|1 - r_{\text{mass}}|$ as measured on the sequence of grids for the selected discretization methods, are given in Figure 15.6. Classifications are given in Table 15.7. In this table, per method, we give the aforementioned order-of-accuracy difference $p_{|1-r_{\text{mass}}|} - p_{\|\Delta c\|_1}$, where $p_{\|\Delta c\|_1}$ has already been given in Table 15.5.

Schemes of which the order of $|1 - r_{\text{mass}}|$ behaves clearly less well than that of $\|\Delta c\|_1$, are: the second-moment, leap-frog, MFCT, and ENO schemes. All remaining schemes behave well. Still note the good convergence of the narrow scheme. This good performance is explained by the low crosswind-diffusion of that scheme.

Table 15.7: Classifications of discretization methods with respect to $|1 - r_{\text{mass}}|$

error level		*error convergence*	
method	$\overline{\lvert 1 - r_{\text{mass}} \rvert}$	*method*	$p_{\lvert 1-r_{\text{mass}} \rvert} - p_{\lVert \Delta c \rVert_1}$
SGA/CN-consistent	9.0×10^{-6}	cyclic	2.0
adjoint-equation	9.2×10^{-5}	narrow	1.0
second-moment	2.9×10^{-4}	adjoint-equation	0.6
cyclic	1.5×10^{-3}	SEM, skew-triangle	0.5
ENO-4-LF	4.6×10^{-3}	limited - $\kappa = \frac{1}{3}$	0.0
limited - $\kappa = \frac{1}{3}$	5.9×10^{-3}	SGA/CN-consistent	-0.3
MFCT	6.0×10^{-3}	ENO-4-LF	-1.1
leap-frog	1.6×10^{-2}	MFCT	-1.3
narrow	5.5×10^{-2}	leap-frog	-2.2
SEM	6.8×10^{-2}	second-moment	-2.4
skew-triangle	3.7×10^{-1}		

15.2.5 Synopsis

Table 15.8 collects all preceding classifications of accuracy, efficiency, positivity, and conservation. Here ++ may be interpreted as very good, + as good, and − as less good. In the evaluation of accuracy versus computational efficiency, the two semi-Lagrangian schemes and the narrow scheme have been left out for reasons explained in Section 15.2.2.

15.3 Evaluation numerical results Problems 1, 2, 3.1, and 3.2

Extensive quantitative evaluations are not possible for these four 1-D problems (because no explicit request has been made for quantitative results, and also because no specific grid sequences have been prescribed). Nevertheless, some interesting partly quantitative - partly qualitative comparisons can be made. In the following, per problem, we look for (as far as we can judge) the 'best' method per chapter, and give qualifications on such properties as accuracy (phase errors, resolution of maxima, shocks, ...) and monotonicity (or, if applicable, positivity). Chapter 11 is left out here, since it considers multi-D methods and multi-D problems only.

15.3.1 Problem 1

First, in Table 15.9 (in the 3rd-5th column), we give our evaluation of numerical results obtained for Problem 1. (In most cases, the name of a method in Table 15.9 refers to the discretization scheme applied to the advection operator.) The same qualifications are used as before (++: very good, +: good, −: less good). In the last column, as far as available, we also give the order of accuracy with respect to $\|\Delta c\|_1$, as measured from the one-but-finest to the finest grid.

An interesting feature of Problem 1 is that its initial condition has a discontinuous first derivative at two points. Due to these two kinks in the initial solution, no higher than $\mathcal{O}(h^2)$ $\|\Delta c\|_1$ convergence can be expected because, in general, a kink in the initial solution causes an $\mathcal{O}(h)$ error extending over an $\mathcal{O}(h)$ area. Note that the presence of

Table 15.8: Specific discretization methods and their evaluation for Problem 4

Chapter	*method*	*accuracy*	*accuracy versus CPU-time*	*positivity*	*conservation*
2	leap-frog	+	+	−	−
3	skew-triangle	−	−	++	−
3	cyclic	+	++	−	+
4	MFCT	+	+	++	−
5	limited - $\kappa = \frac{1}{3}$	+	+	+	+
6	ENO-4-LF	++	+	+	−
7	SEM	++	+	−	+
8	SGA/CN-consistent	++	+	−	++
9	adjoint-equation	++	left out	++	++
10	second-moment	++	left out	++	+
11	narrow	−	left out	++	+

Table 15.9: Specific discretization methods and their evaluation for Problem 1

method	*Figure*	*phase*	*maximum*	*positivity*	$p_{\|\Delta c\|_1}$
leap-frog	2.17b	+	++	−	3.7
quadratic upwind	3.7	−	+	−	2.0
cyclic	3.29	+	++	−	1.9
MFCT	4.3	++	+	+	2.5
limited - $\kappa = \frac{1}{3}$	5.9	++	+	++	2.9
upwind biased ENO-6	6.2d	++	++	++	see discussion in Section 6.3
SEM	7.6	++	++	+	·
SGA-consistent	8.2	++	++	+	·
adjoint-equation	9.4	++	++	++	3.1
second-moment	10.11	++	++	++	2.0

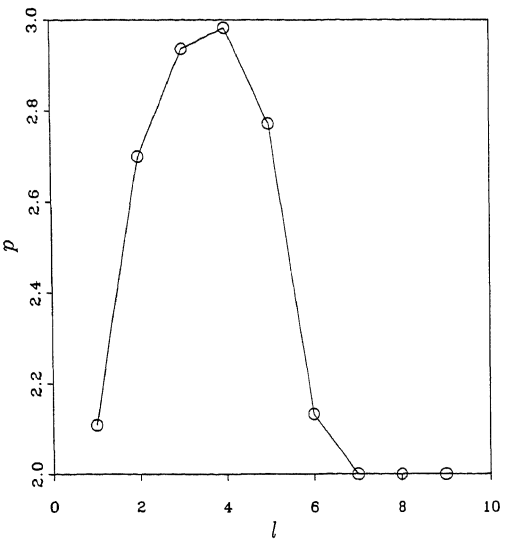

Figure 15.7: Orders of $\|\Delta c\|_1$-accuracy measured for Problem 1 on an extensive sequence of grids, for third-order accurate space discretization

diffusion cannot help to remove the $\mathcal{O}(h^2)$ $\|\Delta c\|_1$-error made in discretizing the initial solution. (Diffusion does make the exact solution C^∞ at $t = 0^+$; if the time integration were started from that moment, there would be no $\mathcal{O}(h^2)$ order barrier.) In spite of this theoretical $\mathcal{O}(h^2)$ order barrier, for the grids considered some of the $\mathcal{O}(h^p)_{p>2}$ methods still seem to reach their theoretical order of accuracy, valid for perfectly smooth problems. However, in Section 6.3, for the present problem Walsteijn pointed out the feature that for $\mathcal{O}(h^p)_{p>2}$ methods, after a "pre-asymptotic" convergence to their corresponding theoretical $\mathcal{O}(h^p)$ (valid for perfectly smooth problems), the orders finally converge to the expected $\mathcal{O}(h^2)$. To show this "pre-asymptotic" convergence, in Figure 15.7 we depict the orders of $\|\Delta c\|_1$-accuracy, as measured on a very extensive sequence of grids, by means of a finite-difference space discretization which is formally third-order accurate for the advective part (a non-limited - $\kappa = \frac{1}{3}$ discretization), and fourth-order accurate for the diffusive part (standard $\mathcal{O}(h^4)$ central). Time integration is done through the standard, fourth-order accurate Runge-Kutta scheme, with the time step Δt in linear proportion to the mesh size and sufficiently small to ensure that time discretization errors are negligible with respect to space discretization errors. In Figure 15.7, grid level l corresponds to the grid with $2^l \times 20$ (interior) grid points. Indeed, it appears that $\mathcal{O}(h^3)$ convergence sets in at first, but that at enhanced grid refinement, $\|\Delta c\|_1$ finally converges as $\mathcal{O}(h^2)$. It is remarkable that the "pre-asymptotic" $\mathcal{O}(h^3)$ accuracy collapses where the cell Péclet number $P = \frac{uh}{D}$ passes 1: from $l = 4$ to $l = 5$. As soon as P has become smaller than 1, for reasons of accuracy, it is expected that Δt should be taken proportional to h^2 (instead of proportional to h, as we did). A conjecture might be that not obeying this quadratic proportionality is a secondary cause of the order reduction. However, additional numerical experiments with Δt in proportion to h^2 have shown that this conjecture is false; in going from $l = 4$ to $l = 5$, the identical collapse of $p_{\|\Delta c\|_1}$

Table 15.10: Specific discretization methods and their evaluation for Problem 2

method	*Figure*	*maximum*	*wake*	*positivity*	$p_{\|\Delta c\|_1}$
compact RK4	2.19c	++	++	++	2.0
quadratic upwind	3.13	+	+	++	1.9
cyclic	3.33	++	++	+	0.6
MFCT	4.7	++	+	+	2.6
limited - $\kappa = \frac{1}{3}$	5.13	++	++	++	1.9
ENO-6	6.3b	++	++	++	·
SEM	7.3	++	+	+	·
SGA	8.5	++	+	−	·
adjoint-equation	9.6	++	+	−	1.1
second-moment	10.12	++	+	−	1.7

occurred. The explanation for the "pre-asymptotic" convergence to higher than $\mathcal{O}(h^2)$ accuracy is that at first, (i.e. on the coarser meshes) the kinks are not yet clearly 'visible', and hence - at first - there is no reduction of accuracy.

The present results suggest that $\mathcal{O}(h^p)_{p>2}$ discretization methods are of limited practical importance to pollutant-transport problems, since non-smooth initial solutions are very common in these problems.

15.3.2 Problem 2

In Table 15.10 (in the 3rd-5th column), the qualitative evaluation for Problem 2 is given. We also look at qualitative solution accuracy in the wake of the source. (Uncareful treatment of the two discontinuities in the source is expected to show up in the wake.) In the last column we give again orders of accuracy with respect to $\|\Delta c\|_1$. It is to be expected that local $\mathcal{O}(h)$ errors occur near the two jumps; $\|\Delta c\|_1$ will then behave $\mathcal{O}(h^2)$ at most.

As opposed to the accuracy results observed for Problem 1 (Table 15.9, last column), here it appears that not till very fine, but already on the present moderately fine grids, most of the numerical methods do *not* reach higher than second-order accuracy. (Only the MFCT scheme does.) Since discontinuous source terms may also often occur in pollutant-transport problems, this probable accuracy barrier suggests that $\mathcal{O}(h^p)_{p>2}$ discretization methods might be of limited importance to these problems as well.

15.3.3 Problem 3.1

For Problem 3.1 we confine ourselves to a qualitative evaluation only (Table 15.11). Unfortunately, no cyclic scheme has been applied to this nonlinear problem, nor to Problem 3.2. Instead of positivity we consider monotonicity. As expected, the monotonicity property has become more discriminating here than it was for the previous linear problems. The results in Table 15.11 speak for themselves.

15.3.4 Problem 3.2

In Table 15.12, the evaluation for Problem 3.2 is given. Except for the local maximum, the same properties are considered as for Problem 3.1. (Instead of the local maximum,

Table 15.11: Specific discretization methods and their evaluation for Problem 3.1

method	*Figure*	*phase*	*maximum*	*monotonicity*
compact RK4	2.13	++	++	+
quadratic upwind	3.16	+	+	−
MFCT	4.11	++	+	+
limited - $\kappa = \frac{1}{3}$	5.5	++	+	++
ENO-4	6.4d	++	++	++
SEM	7.7	++	++	−
SGA	8.7	++	++	+
adjoint-equation	9.7	+	+	−
second-moment	10.13	++	++	−

Table 15.12: Specific discretization methods and their evaluation for Problem 3.2

method	*Figure*	*phase*	*steepness*	*monotonicity*
Lax-Wendroff	2.12	++	++	−
first-order upwind	3.17	++	++	−
MFCT	4.14	++	++	+
limited - $\kappa = \frac{1}{3}$	5.6	++	++	++
ENO-4	6.6d	++	++	++
SEM-Picard	7.8	+	+	+
SUPG	8.9	++	++	−
adjoint-equation	9.8+9.9	+	+	+
second-moment	10.14	++	++	+

we look at the steepness of the discontinuity.) The monotonicity property has become even more discriminating here.

Remarkable are the very small phase errors shown by almost all methods. As discussed in Chapter 1, use of the non-conservative form of the equation may lead to erroneous shock solutions. Surprisingly, this does not even occur with the spectral-element method which is explicitly in non-conservative form. As expected, the streamline upwind Petrov-Galerkin finite-element scheme performs better for this non-smooth problem than does the standard Galerkin finite-element scheme. (We remark that the streamline upwind Petrov-Galerkin scheme applied here is not a specifically tailored method, but - instead - a generally applicable method.) The unexpected monotonicity which arises in the first-order upwind results from Chapter 3, is caused by a central evaluation of the term c^4 in the quasi-linear form of the equation (see Section 3.2.4).

Because, in general, an $\mathcal{O}(1)$ solution error will occur at the shock, a higher than $\mathcal{O}(h)$ convergence of $\|\Delta c\|_1$ generally cannot be expected. Despite of this severe order barrier, the order of accuracy is still of interest here. For linear shock propagation, it can be argued that a p-th order method yields an $\mathcal{O}(\frac{p}{p+1})$ $\|\Delta c\|_1$-convergence. To give some evidence of this, consider the equation

$$\frac{\partial c}{\partial t} + u\frac{\partial c}{\partial x} = 0, \tag{15.4}$$

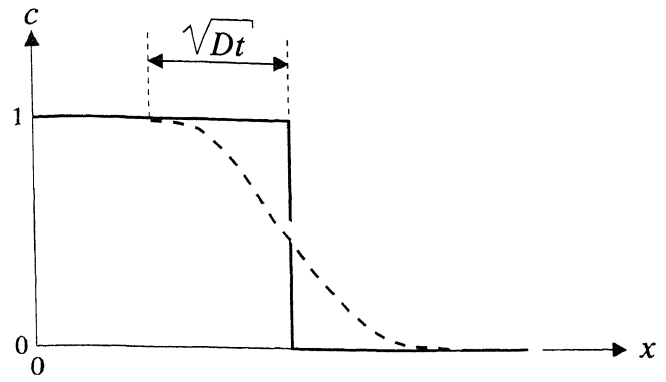

Figure 15.8: Exact solution and solution of first-order accurate upwind discretization; linear advection equation with discontinuous initial solution

with the initial solution

$$\begin{aligned} c(x, t = 0) &= 1 \quad x \leq 0, \\ c(x, t = 0) &= 0 \quad x > 0. \end{aligned} \tag{15.5}$$

It is known (see e.g. [1, 2]) that the standard first-order accurate upwind scheme yields a solution which approximately satisfies the modified equation

$$\frac{\partial c}{\partial t} + u\frac{\partial c}{\partial x} = D\frac{\partial^2 c}{\partial x^2}, \tag{15.6}$$

where $D = \mathcal{O}(h)$. Both (15.4) and (15.6) can be solved exactly. Then $\|\Delta c\|_1$ can be determined. It is found to behave as $\mathcal{O}(\sqrt{Dt})$ (Figure 15.8), i.e. (with $D = \mathcal{O}(h)$) as $\mathcal{O}(\sqrt{h})$. A similar reasoning for a second-order accurate space discretization leads to an $\mathcal{O}(h^{\frac{2}{3}})$ convergence of $\|\Delta c\|_1$. In general, for an $\mathcal{O}(h^p)$ space discretization and a linear shock problem, an $\mathcal{O}(1)$ error will be committed at the shock, whereas the region over which this error spreads will have an $\mathcal{O}(Dt)^{\frac{1}{p+1}}$ width. As a consequence, one gets an $\mathcal{O}\left(h^{\frac{p}{p+1}}\right)$ $\|\Delta c\|_1$-convergence. A similar analysis for the nonlinear advection equation

$$\frac{\partial c}{\partial t} + \frac{\partial (c^n)}{\partial x} = 0, \tag{15.7}$$

would be of interest. It might well show that for Problem 3.2, $\|\Delta c\|_1$ converges faster than $\mathcal{O}(h^{\frac{p}{p+1}})$ (but still slower than $\mathcal{O}(h)$, of course). With increasing nonlinearity, the region in which the error occurs (Figure 15.8) is expected to be compressed.

In conclusion, we remark that a *non-scalar* variant of this problem would have been more discriminating, for, whereas in a scalar problem numerical errors entering the shock are 'swallowed' by it, in a non-scalar problem such errors may come out of it again.

15.4 Conclusions

A rather wide variety of discretization methods for advection-diffusion equations has been evaluated: finite-difference, finite-volume, finite-element, spectral-element, semi-Lagrangian, and fluctuation-splitting methods; central and upwind methods; conservative and non-conservative methods; linear and nonlinear methods; and so on. Among all discretization methods considered, the "ultimate" method has not been found, though for the prescribed set of test problems a few methods come very close.

For a possible future evaluation, we suggest that test problems are prescribed which are of a more large-scale nature. We are thinking of e.g. 2-D boundary-layer problems, 2-D nonlinear advection problems, and 3-D linear advection problems. The advantage of 'large-scaleness' is the increased importance of computational efficiency; the choice (or construction) of the combination 'discretization method + solution method' will be more critical then. As for the present book we hope that sufficient material has been presented in it to help users to select methods which meet most of their requirements.

Acknowledgment

J.C.H. van Eijkeren, B. van Leer, R. Struijs, and F.H. Walsteijn are acknowledged for their suggestions in improving this chapter.

References

[1] LEVEQUE, R.J.: *Numerical Methods for Conservation Laws* (Birkhäuser, Basel, 1990).

[2] STRIKWERDA, J.C.: *Finite Difference Schemes and Partial Differential Equations* (Wadsworth and Brooks/Cole, Pacific Grove, California, 1989).